tive and not necessarily inconsistent model suggests that a molecular target is the TATA-binding factor TFIID (*13*). The VP16 activation domain selectively and directly binds yeast and human TFIID polypeptides in vitro (*14*). Furthermore, the affinity of in vitro binding of TFIID by various VP16 derivatives (*15*) correlates with the activity of the VP16 activation domain in vivo. These results strongly suggest that the mechanism of activation by VP16 involves a direct interaction with TFIID.


REFERENCES AND NOTES

1. L. E. Post *et al.*, *Cell* **24**, 555 (1981); M. E. M. Campbell *et al.*, *J. Mol. Biol.* **180**, 1 (1984).
2. T. M. Kristie and B. Roizman, *Proc. Natl. Acad. Sci. U.S.A.* **84**, 71 (1987); S. J. Triezenberg, K. L. LaMarco, S. L. McKnight, *Genes Dev.* **2**, 730 (1988); T. Gerster and R. G. Roeder, *Proc. Natl. Acad. Sci. U.S.A.* **85**, 6347 (1988); C. M. Preston *et al.*, *Cell* **52**, 425 (1988); P. O'Hare and C. R. Goding, *ibid.*, p. 435; C. I. Ace, M. A. Dalrymple, F. H. Ramsay, V. G. Preston, C. M. Preston, *J. Gen. Virol.* **69**, 2595 (1988); G. Werstuck and J. P. Capone, *Gene* **75**, 213 (1989); *J. Virol.* **63**, 5509 (1989); R. F. Greaves and P. O'Hare, *ibid.* **64**, 2716 (1990).
3. S. J. Triezenberg, R. C. Kingsbury, S. L. McKnight, *Genes Dev.* **2**, 718 (1988).
4. R. Greaves and P. O'Hare, *J. Virol.* **63**, 1641 (1989).
5. I. Sadowski *et al.*, *Nature* **335**, 563 (1988).
6. D. J. Cousens, R. Greaves, C. R. Goding, P. O'Hare, *EMBO J.* **8**, 2337 (1989).
7. I. A. Hope and K. Struhl, *Cell* **46**, 885 (1986); J. Ma and M. Ptashne, *ibid.* **48**, 847 (1987); S. L. Forsburg and L. Guarente, *Genes Dev.* **3**, 1166 (1989); P. J. Godowski, D. Picard, K. R. Yamamoto, *Science* **241**, 812 (1988).
8. E. Giniger and M. Ptashne, *Nature* **330**, 670 (1987); M. Ptashne, *ibid.* **335**, 683 (1988).
9. W. D. Cress and S. J. Triezenberg, unpublished data.
10. P. J. Mitchell and R. Tjian, *Science* **245**, 371 (1989).
11. A. J. Courey and R. Tjian, *Cell* **55**, 887 (1988).
12. B. F. Pugh and R. Tjian, *ibid.* **61**, 1187 (1990); S. L. Berger, W. D. Cress, A. Cress, S. J. Triezenberg, L. Guarente, *ibid.*, p. 1199; R. J. Kelleher *et al.*, *ibid.*, p. 1209; F. Liu and M. R. Green, *ibid.*, p. 1217.
13. M. Horikoshi, M. F. Carey, H. Kakidani, R. G. Roeder, *ibid.* **54**, 665 (1988); M. Horikoshi, T. Hai, Y.-S. Lin, M. R. Green, R. G. Roeder, *ibid.*, p. 1033; T. Hai *et al.*, *ibid.*, p. 1043.
14. K. F. Stringer *et al.*, *Nature* **345**, 783 (1990).
15. C. J. Ingles, M. Shales, W. D. Cress, S. J. Triezenberg, J. Greenblatt, in preparation.
16. Single letter abbrevations for the amino acids are A, Ala; C, Cys; D, Asp; E, Glu; F, Phe; G, Gly; H, His; I, Ile; K, Lys; L, Leu; M, Met; N, Asn; P, Pro; Q, Gln; R, Arg; S, Ser; T, Thr; V, Val; W, Trp; and Y, Tyr.
17. M. J. Zoller and M. Smith, *Nucleic Acids Res.* **10**, 6487 (1982); T. A. Kunkel, *Proc. Natl. Acad. Sci. U.S.A.* **82**, 488 (1985).
18. B. J. Graves, R. N. Eisenman, S. L. McKnight, *Mol. Cell. Biol.* **5**, 1948 (1985).
19. J. Devereux, P. Haeberli, O. Smithies, *Nucleic Acids Res.* **12**, 387 (1984).
20. N. Mermod *et al.*, *Cell* **58**, 741 (1989).
21. J. Ma and M. Ptashne, *ibid.* **51**, 113 (1987).


22. We thank A. Cress, J. Regier, and R. Pichyangkura for thoughtful suggestions and enthusiastic assistance and C. J. Ingles, S. L. Berger, S. L. McKnight, Z. Burton, and L. Kroos for helpful discussions and for critically reading the manuscript. Supported by funds from Michigan State University, the Michigan Agricultural Experiment Station, NIH grant AI 27323, and a Barnett Rosenberg Graduate Fellowship (W.D.C.).

23 July 1990; accepted 1 November 1990


# Three-Dimensional Structures of Acidic and Basic Fibroblast Growth Factors


X. ZHU, H. KOMIYA, A. CHIRINO, S. FAHAM, G. M. FOX, T. ARAKAWA, B. T. HSU, D. C. REES*



**Members of the fibroblast growth factor (FGF) family of proteins stimulate the proliferation and differentiation of a variety of cell types through receptor-mediated pathways. The three-dimensional structures of two members of this family, bovine acidic FGF and human basic FGF, have been crystallographically determined. These structures contain 12 antiparallel β strands organized into a folding pattern with approximate threefold internal symmetry. Topologically equivalent folds have been previously observed for soybean trypsin inhibitor and interleukins-1β and -1α. The locations of sequences implicated in receptor and heparin binding by FGF are presented. These sites include β-sheet strand 10, which is adjacent to the site of an extended sequence insertion in several oncogene proteins of the FGF family, and which shows sequence conservation among the FGF family and interleukin-1β.**


FIBROBLAST GROWTH FACTORS (FGFs) are members of a protein family that induce mitogenic, chemotactic, and angiogenic activity in a variety of cells of epithelial, mesenchymal, and neural origins (*1*). As a consequence of their strong affinity for heparin, FGFs are also referred to as heparin-binding growth factors (HBGFs). Interests in FGFs have centered on the molecular details of the receptor-mediated pathways by which their diverse physiological activities are expressed and the design of therapeutically useful agents that could either mimic or inhibit the action of these growth factors. Acidic FGF (aFGF) and basic FGF (bFGF), two original members of the FGF family, have similar but distinguishable biological activities and exhibit approximately 55% sequence identity (*2, 3*). Five other members of the FGF family have been presently identified on the basis of sequence homology and the ability to modulate cell proliferation and differentiation: four are putative oncogene products [int-2 (*4*), hst/KS3 (*5*), FGF-5 (*6*), and FGF-6 (*7*)], and the fifth is keratinocyte growth factor (*8*). A three-dimensional model for a member of the FGF family would provide a structural framework for discussing the relation between these different proteins and for identifying the spatial locations of residues involved in receptor and heparin binding. In this report we describe the crystallographic structures for both aFGF and bFGF. Strikingly, the FGF family exhibits a folding pattern similar to that observed for the cytokines interleukins-1α and -1β (IL-1α and IL-1β).


X. Zhu, H. Komiya, A. Chirino, S. Faham, B. T. Hsu, D. C. Rees, Division of Chemistry and Chemical Engineering, California Institute of Technology, Pasadena, CA 91125.
G. M. Fox and T. Arakawa, Amgen, Thousand Oaks, CA 91320.

*To whom correspondence should be addressed.


A recombinant analog of bovine aFGF (*9*), in which $Cys^{47}$ and $His^{93}$ were changed to Ala and Gly, respectively, was used in this study. The biological activity of this analogue is equal to or greater than the corresponding natural sequence molecule either with or without heparin. Crystals were grown by vapor diffusion against 0.2 M $(NH_4)_2SO_4$, 2 M NaCl, 0.099 M sodium citrate, and 0.02 M sodium potassium phosphate, pH 5.6. The protein droplet contained equal volumes of the reservoir solution and a 10 mg/ml protein solution. The crystals are trigonal (space group $P3_121$, $a$ = 78.6 Å and $c$ = 115.9 Å) and diffract to 2.5 Å resolution. Intensity data were collected with a Siemens multiwire area detector mounted on an 18-kW rotating-anode generator. The XENGEN (*10*) and ROCKS (*11*) crystallographic packages were used for data reduction and processing. Multiple isomorphous replacement (MIR) phases were calculated to 3 Å resolution from two derivatives, ethylmercurithiosalicylate (EMTS) and $K_2PtCl_4$, with a figure of merit of 0.68 (Table 1). After solvent flattening (*12*), regions corresponding to two independent aFGF molecules in the asymmetric unit were identified. The general noncrystallographic symmetry relations between these molecules were determined from rotation function, real-space translation function, and density correlation studies (*13–15*). A molecular envelope was defined around an averaged aFGF molecule by a modification of the Wang algorithm (*12*). Phases were then iteratively refined by molecular averaging and solvent flattening (*14*). Initial maps revealed extended regions of β-sheet structure that were truncated at the loops because the molecular envelope was too small. The final map for model building was calculated with MIR phases [from heavy-atom parameters rerefined against averaged phases, as described in (*16*)] and iteratively averaged

with a molecular envelope generated by placing 3 Å spheres about the atomic positions in the initial model. Averaging at 3 Å resolution converged to a final $R$ factor of 0.183 between the observed structure factors ($F_o$) and the structure factors calculated from the averaged and solvent flattened map ($F_c$). The graphics program TOM/FRODO (*17*), implemented for a Silicon Graphics 4D80 by C. Cambillau, was used to build residues a1 to a137 of the aFGF sequence into the averaged electron density map. Residue numbers of aFGF correspond to the mature bovine sequence (*2*) and are prefixed with "a." The amino-terminal residues a1 to a9 were disordered in one of the two crystallographically independent aFGF molecules. Refinement of the aFGF model (without solvent molecules) with the programs PROLSQ (*18*) and XPLOR (*19*) has currently progressed to an $R$ factor of 0.209 ($R = \Sigma|F_o - F_c|/\Sigma F_o$) between 8.0 to 2.7 Å resolution, with root-mean-square (rms) deviations from ideal bond distances and angles of 0.02 Å and 3.8°, respectively.

Crystals of recombinant human bFGF [with cysteines at residues 70 and 88 replaced by serines (*20*)] were grown by vapor diffusion against 25% polyethylene glycol 8000, 5% methylpentanediol, and 0.1 M Hepes, pH 7.6. The protein droplet contained equal volumes of the reservoir solution and a 9 mg/ml bFGF solution. The crystals grow in space group $P1$, $a$ = 31.1 Å, $b$ = 33.5 Å, $c$ = 37.0 Å, $\alpha$ = 64.2°, $\beta$ = 106.4°, and $\gamma$ = 103.3°, and diffract to beyond 1.7 Å resolution. The origin of the $P1$ unit cell was assigned by positioning an aFGF molecule in the bFGF cell (with an orientation determined from a rotation function calculation), so that the origin of the bFGF unit cell approximately coincides with the center of mass of the aFGF molecule. Heavy-atom positions in the bFGF crystal were determined by difference Fourier calculations with these molecular replacement phases. Isomorphous replacement phases were calculated to 2.8 Å (figure of merit = 0.62) with the same two derivatives used for the aFGF structure (Table 1). The resulting MIR electron density map revealed similar molecular folds for both aFGF and bFGF, and the aFGF structure was used as the starting model to build residues b20 to b144 of bFGF into the electron density map with TOM/FRODO. Extra density for the 19 residues at the amino terminus is present, but we have so far been unable to satisfactorily model the sequence in this region. Residue numbers of bFGF correspond to the recombinant protein sequence (*20*), prefixed with "b." The bFGF residue numbers are one greater than in the protein sequence (*3*) because of the presence of an amino-terminal methionine in the recombinant sequence. Residue numbers referred to below have been accordingly adjusted. The sequence relations between aFGF and bFGF are such that residue numbers up to b114 are ten greater than the corresponding aFGF numbers; after residue b114, the difference is eight. Refinement of the bFGF model (without solvent molecules) by the molecular dynamics program XPLOR (*19*) has currently progressed to an $R$ factor of 0.224 between 5.0 to 1.9 Å

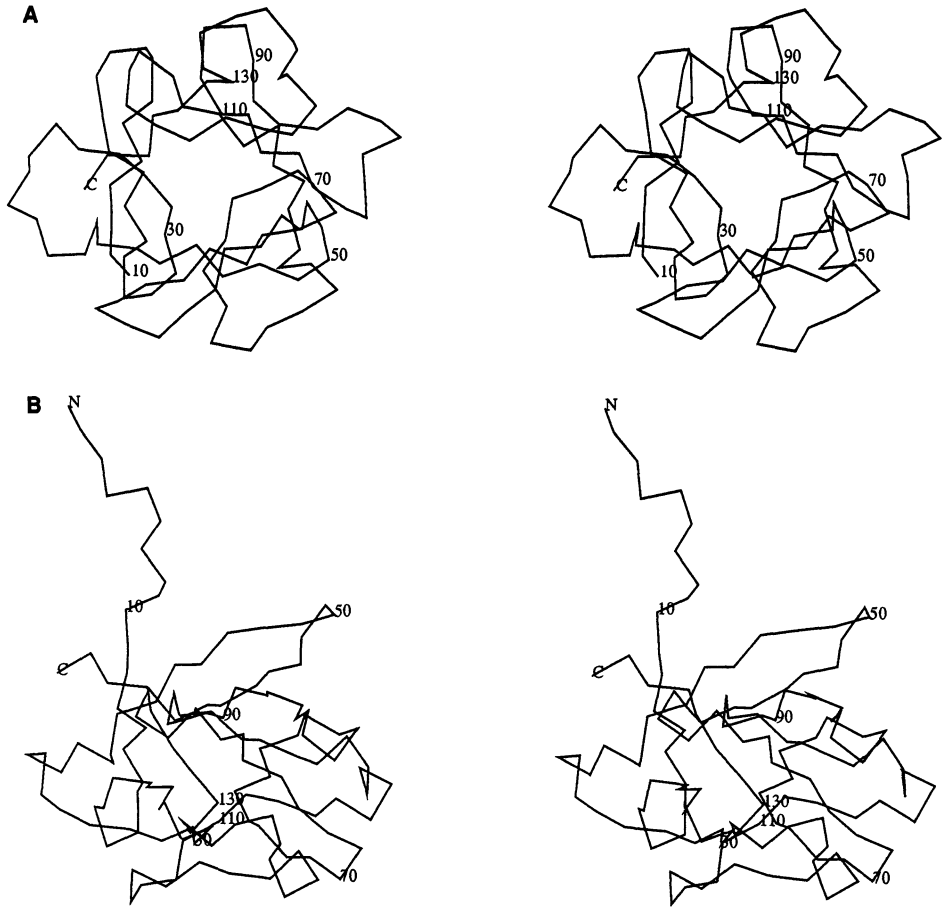


**Fig. 1.** (**A**) Stereoview of Cα trace of residues a10 to a136 aFGF viewed down the internal threefold symmetry axis. (**B**) Stereoview of the Cα trace of residues a1 to a137 of aFGF viewed with the internal threefold symmetry axis in the vertical plane of the page. The conformation of residues a1 to a9 is stabilized by lattice contacts and is observed in only one of the two crystallographically independent aFGF molecules.

**Table 1.** Heavy-atom sites and phasing information. The absolute hand of the aFGF structure was established by using anomalous differences measured for the EMTS derivative. The phasing powers, $f_H/E$, were 2.0 and 1.0 for the EMTS and $K_2PtCl_4$ derivatives of aFGF to 3.0 Å, respectively, and 2.0 and 2.2 for the EMTS and $K_2PtCL_4$ derivatives of bFGF to 2.8 Å, respectively. Native aFGF, EMTS, and $K_2PtCl_4$ data sets were 93, 75, and 75% complete to 3.0 Å, respectively, and the native bFGF, EMTS, and $K_2PtCl_4$ data sets were 99.8, 87, and 91% complete to 2.8 Å resolution, respectively.

| Derivative | Soak | $x$ | $y$ | $z$ | Occupancy | Location |
|---|---|---|---|---|---|---|
| | | | *aFGF* | | | |
| EMTS | 4 mM, 12 hours | 0.545 | 0.344 | 0.0149 | 0.47 | $Cys^{a83}$, molecule 1 |
| $K_2PtCl_4$ | 3.3 mM, 7 days | 0.111 | 0.872 | 0.0460 | 0.36 | Amino-terminal Met, molecule 2 |
| | | 0.555 | 0.355 | 0.0190 | 0.26 | $Cys^{a83}$, molecule 1 |
| | | 0.147 | 0.548 | 0.1450 | 0.14 | $His^{a124}$, molecule 1 |
| | | | *bFGF* | | | |
| EMTS | 3 mM, 3 days | 0.245 | 0.820 | 0.294 | 0.73 | $Cys^{b93}$ |
| $K_2PtCl_4$ | 5 mM, 2 days | 0.716 | 0.153 | 0.597 | 0.53 | $Met^{b143}$ |
| | | 0.448 | 0.066 | 0.735 | 0.31 | $His^{b36}$ |
| | | 0.323 | 0.871 | 0.748 | 0.30 | $His^{b51}$ |
| | | 0.106 | 0.714 | 0.767 | 0.28 | Amino-terminal region, not yet identified |

resolution, with rms deviations from ideal bond distances and angles of 0.01 Å and 3.1°, respectively.

The correctness of the FGF chain traces are supported by differences in side-chain densities for aFGF and bFGF that are consistent with a sequence alignment of the two proteins, including insertions and deletions, and the involvement of appropriate amino acid side chains in the heavy-atom binding sites (Table 1). Overall, the three independently determined FGF structures (two aFGF molecules and one bFGF) are quite similar; chief differences are in the ordering of the nine residues at the amino terminus in only one of the two aFGF molecules and the deletion of two residues in bFGF corresponding to a105 and a106 in a turn between two β strands. A more quantitative analysis of the relation between the different FGF structures must await completion of the coordinate refinement.

The aFGF and bFGF structures consist of 12 antiparallel β strands arranged in a pattern with approximate threefold internal symmetry (Fig. 1). The strands are numbered sequentially from the amino terminus. β Strands 1, 4, 5, 8, 9, and 12 form a six-stranded antiparallel β barrel that is closed at one end by β sheet interactions involving strands 2, 3, 6, 7, 10, and 11. Rather extended loops occur between strands β3 and β4, β7 and β8, and β11 and β12. The internal symmetry relates strands 1 to 4, 5 to 8, and 9 to 12. A striking feature of the aFGF-bFGF structures is the overall similarity to the folding pattern observed for the interleukins IL-1β and IL-1α (*19–22*). The similarity between the FGF and IL-1 folds was previously suggested on the basis of weak but detectable similarities between the sequences (*2*). This common fold was originally observed in the structure of soybean trypsin inhibitor (Kunitz) (*23, 24*). Following MacLachlan (*24*), each repeating unit of four β strands and a loop is designated as a lobe, and the three copies of this motif are labeled I, II, and III. Amino acid sequences in topologically equivalent regions of aFGF and IL-1β [coordinate set 4I1B of the Brookhaven Protein Data Bank (*21*)] were structurally aligned by manual superposition of the Cα traces of the two proteins with the FBRT option of TOM/FRODO (Fig. 2). The resulting alignments for residues in the β strand regions of aFGF, bFGF, and IL-1β are presented in Table 2. Alignment of loop residues in different lobes was not possible given the variation in conformation and the number of residues. Despite the structural equivalence of the lobes, there appears to be little accompanying sequence similarity either within a given protein or between FGF and IL-1β. This situation obviously complicates sequence alignment in the absence of a structure. While the homology between FGF and IL-1β was predicted by sequence analysis (*2*), significant discrepancies are evident in the sequence and structural alignments, with the exception of the region near β9 and β10.

**Table 2.** Structural alignment of β strands in aFGF, bFGF, and IL-1β (*30*). The repeating units of these structures are designated I, II, and III, where I contains β1-β4, II contains β5-β8, and III contains β9-β12. The Cα atoms of equivalent residues were generally separated by less than 2 Å after manual superposition of the structures. The greatest differences between aFGF and IL-1β were observed in β2, β3, and β11, where deviations exceeded 2 Å.

| Protein/ unit | β Strands | | | | | | | |
|---|---|---|---|---|---|---|---|---|
| | 1 | | 2 | | 3 | | 4 | |
| aFGF/I | a11 | PKLLYCS* | a21 | YFLRIL* | a30 | TVDGT | a42 | IQLQLAA* |
| II | a53 | EVYIKST | a63 | QFLAMD | a72 | LLYGS | a83 | CLFLERL |
| III | a94 | YNTYISK | a107 | WFVGLK | a116 | RSKLG | a130 | ILFLPLP |
| bFGF/I | b21 | PKRLYCK | b31 | FFLRIH | b40 | RVDGV | b52 | IKLQLQA |
| II | b63 | VVSIKGV | b73 | RYLAMK | b82 | RLLAS | b93 | CFFFERL |
| III | b104 | YNTYRSR | b115 | WYVALK | b124 | QYKLG | b138 | ILFLPMS |
| IL-1 β/I | 7 | NCTLRDS | 16 | KSLVMS | 25 | ELKAL | 40 | VVFSMSF |
| II | 57 | PVALGLK | 67 | LYLSCV | 79 | TLQLE | 99 | FVFNKIE |
| III | 109 | KLEFESA | 120 | WYISTS | 131 | PVFLG | 144 | TDFTMQF |

*Designates core residues packed around the internal symmetry axis.

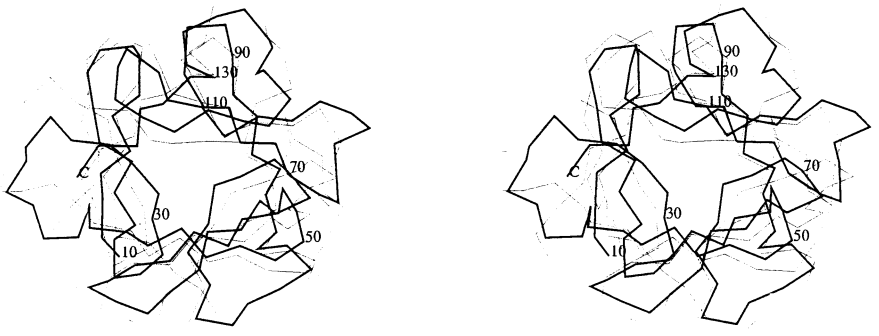


**Fig. 2.** Stereoview of the superposition of the Cα traces of aFGF (thick lines) and IL-1β (thin lines). The view is down the internal symmetry axis.

Although the sequence similarity between lobes is low, the hydrophobic character of residues at several positions in the β sheets is strongly conserved in the FGF–IL-1β sequences. Residues of aFGF, bFGF, and IL-1β in lobes I, II, and III at positions corresponding to a14, a23, and a44 are primarily either Leu, Ile, or Phe, with a single occurrence each of Tyr and Val (Table 2). Examination of the FGF structures shows that residues in these nine positions form the hydrophobic core of the molecule, and are situated around the internal threefold axis. Packing and hydrophobicity constraints apparently more severely restrict substitution at these positions, compared to most other residues in FGF–IL-1β.

Several regions of the FGF sequence have been identified as participating in (i) receptor binding, (ii) heparin binding, and (iii) nuclear translocation. The FGF structures provide a description of the conformation and relative positions of these regions.

Peptides containing residues b25 to b69 and b94 to b121 have been shown to compete with bFGF in a receptor binding assay (*25*). Shorter peptides contained within these sequences, b31 to b51 and b107 to b116, are less effective, but still exhibit significant competition with bFGF for receptor binding (*25*). Peptide b31 to b51 contains strands β2 and β3, while b107 to b116 spans parts of β9 and β10. The corresponding locations of these sequences in the aFGF structure are illustrated in Fig. 3. Consistent with these observations, a recent study of genetically truncated bFGF molecules demonstrated with an in vitro assay that fragments containing b2 to b101 and b42 to b147 (which include the above sequences) can stimulate DNA synthesis by cells (*26*). Furthermore, $Thr^{b113}$, which when phosphorylated by protein kinase A

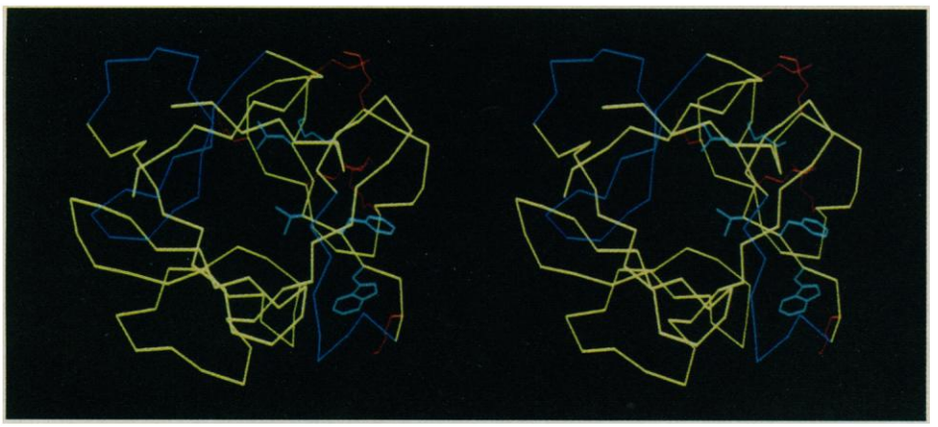

**Fig. 3.** Locations of functionally implicated residues in FGF. Receptor-binding peptides are blue; basic residues between a105 and a128 are red; and residues in strand β10 are cyan. For comparative purposes, residues have been mapped onto aFGF, even when the experimental work involved bFGF.

enhances the binding of bFGF to receptor (*27*), is also located in this general region.

Immediately adjacent to $Thr^{b113}$ is the site of a sequence insertion of 7 to 14 residues in the oncogene proteins int-2 and FGF-5 (*4, 6*). These additional residues can presumably be accommodated in the loop between strands β9 and β10 with minimal consequence on the folding of the remainder of the structure. The location of the insert near the putative receptor-binding site suggests that these residues might directly interact with receptor.

Binding of FGFs to heparin provides not only a convenient purification method but also potentiates their biological activities. Chemical modification (*28*) and thrombin digestion (*29*) studies have implicated $Lys^{a118}$ and $Arg^{a122}$, respectively, in heparin binding. bFGF-related peptides from this region containing residues b94 to b121, b104 to b147, and b106 to b142 have been shown to bind heparin (*25*). Furthermore, the phosphorylation of $Thr^{b113}$ by protein kinase A is blocked in the presence of heparin (*27*). These sequences overlap a basic region of FGF encompassing strands β10 and β11. Seven Lys and Arg residues are contained between a105 to a128 of aFGF, whereas five Lys and Arg residues are present between b115 to b136 of bFGF (Fig. 3). The affinity of this region for anions has been directly demonstrated in the present study by the observation that the major sites of a potential $IrCl_6^{3-}$ heavy atom derivative are adjacent to the side chains of $Lys^{a112}$, $Lys^{a118}$, and $Arg^{a122}$. The possibility exists that additional heparin binding sites may be present, including residues b25 to b69 (*25*). Comparison of the FGF and platelet factor 4 structures (*30*) demonstrates that no unique protein fold is associated with heparin binding.

Recently, the amino-terminal region of aFGF has been demonstrated to function as a nuclear translocation sequence (*31*). This region appears flexible in the FGF crystal structures, as it is disordered in bFGF and one of the two crystallographically independent aFGF molecules. In the second aFGF molecule, residues a1 to a9 are stabilized through contacts with a neighboring molecule in the crystal lattice (Fig. 1B). It therefore appears that the amino-terminal residues of FGF do not specifically interact with the remainder of the molecule, consistent with the observation that this region can be replaced by other nuclear translocation sequences without loss of function (*31*).

Both FGFs and IL-1s are members of a structurally related class of proteins that exhibit cell growth and differentiation activities. The structural similarities suggest that equivalent regions of these proteins might share common functional properties. One such possible region includes residues in and near strand β10 that have been implicated in both receptor and heparin binding and that are adjacent to the sequence insertion found in several FGF-related oncogene proteins (Fig. 3). Strand β10 also contains one of the few tetrapeptide sequences that is reasonably well conserved in both FGFs and IL-1β; this sequence is WYVG in aFGF (a107 to a110), WYVA in bFGF (b115 to b118), and WYIS in IL-1β (120 to 123) (*32*). Both the structural location and the residue conservation suggest that this sequence may be of functional importance. Modification of this region may provide an approach to probe and alter the biological activities of FGFs.

## REFERENCES AND NOTES


1. J. Folkman and M. Klagsbrun, *Science* **235**, 442 (1987); D. Gospodarowicz, N. Ferrara, L. Schweigerer, G. Neufeld, *Endocrinol. Rev.* **8**, 95 (1987); W. H. Burgess and T. Maciag, *Annu. Rev. Biochem.* **58**, 575 (1989); D. Benharroch and D. Birnbaum, *Isr. J. Med. Sci.* **26**, 212 (1990).
2. G. Gimenez-Gallego *et al.*, *Science* **230**, 1385 (1985).
3. F. Esch *et al.*, *Proc. Natl. Acad. Sci. U.S.A.* **82**, 6507 (1985).
4. R. Moore *et al.*, *EMBO J.* **5**, 919 (1986).
5. M. Taira *et al.*, *Proc. Natl. Acad. Sci. U.S.A.* **84**, 2980 (1987); P. Delli-Bovi *et al.*, *Cell* **50**, 729 (1987).
6. X. Zhan, B. Bates, X. Hu, M. Goldfarb, *Mol. Cell Biol.* **8**, 3487 (1988).
7. I. Marics *et al.*, *Oncogene* **4**, 335 (1989).
8. P. W. Finch, J. S. Rubin, T. Miki, D. Ron, S. A. Aaronson, *Science* **245**, 752 (1989).
9. G. M. Fox *et al.*, in preparation.
10. A. J. Howard *et al.*, *J. Appl. Cryst.* **20**, 383 (1987).
11. G. N. Reeke, *ibid.* **17**, 125 (1984); P. H. Bethge, *ibid.*, p. 215.
12. B. C. Wang, *Methods Enzymol.* **115**, 90 (1985).
13. The relative orientations of the two aFGF molecules were established by rotation function studies [M. G. Rossmann and D. M. Blow, *Acta Cryst.* **15**, 24 (1962)] with the use of structure factors calculated from electron density maps masked to contain primarily one molecule. The translational relations were determined by skewing (*14*) the density of one molecule to the same orientation as the second, followed by calculation of a real-space translation function with the use of Fourier coefficients

$$\sum_h [F_o(\bar{h})F_s(h)]e^{-2\pi i h u}$$

where $F_o$ and $F_s$ are the complex structure factors for the observed (MIR) and skewed structures. The rotation and translation parameters were refined by a density correlation method (*15*). The relation between the two molecules is described by the spherical angles $\phi = 47.0°$, $\psi = 81.7°$, and $\kappa = 196.9°$ and a translation of 18.9, 15.6, and 4.6 Å, respectively, in an orthogonal coordinate system defined by *a*, *b**, and *c*.
14. G. Bricogne, *Acta Crystallogr.* **32**, 832 (1976).
15. J. M. Cox, *J. Mol. Biol.* **28**, 151 (1967).
16. M. A. Rould, J. J. Perona, D. Söll, T. A. Steitz, *Science* **246**, 1135 (1989).
17. T. A. Jones, *Methods Enzymol.* **115**, 157 (1985).
18. W. A. Hendrickson, *ibid.*, p. 252.
19. A. T. Brunger, *J. Mol. Biol.* **203**, 803 (1988).
20. G. M. Fox *et al.*, *J. Biol. Chem.* **263**, 18452 (1988).
21. J. P. Priestle, H.-P. Schar, M. G. Grutter, *EMBO J.* **7**, 339 (1988); B. C. Finzel *et al.*, *J. Mol. Biol.* **209**, 779 (1989); B. Veerapandian *et al.*, unpublished coordinate set 4I1B in Brookhaven Protein Data Bank [F. C. Bernstein *et al.*, *J. Mol. Biol.* **112**, 535 (1977)].
22. B. J. Graves *et al.*, *Biochemistry* **29**, 2679 (1990).
23. R. M. Sweet, H. T. Wright, J. Janin, C. H. Chothia, D. M. Blow, *ibid.* **13**, 4212 (1974).
24. A. D. McLachlan, *J. Mol. Biol.* **133**, 557 (1979).
25. A. Baird, D. Schubert, N. Ling, R. Guillemin, *Proc. Natl. Acad. Sci. U.S.A.* **85**, 2324 (1988).
26. M. Seno, R. Sasado, T. Kurokawa, K. Igarashi, *Eur. J. Biochem.* **188**, 239 (1990).
27. J.-T. Feige and A. Baird, *Proc. Natl. Acad. Sci. U.S.A.* **86**, 3174 (1989).
28. J. W. Harper and R. R. Lobb, *Biochemistry* **27**, 671 (1988).
29. R. R. Lobb, *ibid.*, p. 2572.
30. R. St. Charles, D. A. Walz, B. F. P. Edwards, *J. Biol. Chem.* **264**, 2092 (1989).
31. T. Imamura *et al.*, *Science* **249**, 1567 (1990).
32. Abbreviations for the amino acid residues are: A, Ala; C, Cys; D, Asp; E, Glu; F, Phe; G, Gly; H, His; I, Ile; K, Lys; L, Leu; M, Met; N, Asn; P, Pro; Q, Gln; R, Arg; S, Ser; T, Thr; V, Val; W, Trp; and Y, Tyr.


33. Supported by the Beckman Institute and the Joseph Irvine Equipment Fund. D.C.R. is an A. P. Sloan Research Fellow. Coordinates will be deposited in the Brookhaven Protein Data Bank after refinement. Current coordinates may be obtained by sending a tape to D.C.R. or by Bitnet (REES@CITRAY).

19 September 1990; accepted 21 November 1990